Journal of Alloys and Compounds 509 (2011) 2180–2185

Contents lists available at ScienceDirect

Journal of Alloys and Compounds

journal homepage: www.elsevier.com/locate/jallcom

Great influence of a small amount of capping agents on the morphology of SnS particles using xanthate as precursor

Qiaofeng Han*, Meijuan Wang, Junwu Zhu, Xiaodong Wu, Lude Lu, Xin Wang

Key Laboratory for Soft Chemistry and Functional Materials of Ministry Education, Nanjing University of Science and Technology, Nanjing 210094, China

ARTICLE INFO

Article history:
Received 19 July 2010
Received in revised form 26 October 2010
Accepted 28 October 2010
Available online 9 November 2010

Keywords:
Tin sulfide
Crystal growth
Electron microscopy
Microstructure

ABSTRACT

Several hierarchical tin sulfide (SnS) architectures have been prepared based on the reaction of tin dichloride ($SnCl_2 \cdot 2H_2O$) with potassium *O*-ethyldithiocarbonate (ethylxanthate, $C_2H_5OCS_2K$) via a solvothermal route in *N*,*N*-dimethylformamide (DMF) solution at 180 °C for 24 h. By varying experimental parameters such as reaction temperature, reaction time and the ratios of reactants, various morphologies of three-dimensional (3D) superstructures assembled by SnS nanosheets, nanoribbons and nanorods were obtained. The as-prepared products were characterized by X-ray diffraction (XRD), scanning electron microscopy (SEM) and transmission electron microscopy (TEM). For a typical molar ratio of $C_2H_5OCS_2K/SnCl_2 = 2$, the addition of a slight excess of $C_2H_5OCS_2K$ (molar ratio of $C_2H_5OCS_2K/SnCl_2 = 2.4$) resulted in one-dimensional growth of lamellar SnS particles and their assembly into flowerlike superstructures. Similarly, for the molar ratio of $C_2H_5OCS_2K/SnCl_2 = 2$, if a small amount of capping agent (1 mL potassium oleate in 40 mL DMF solution) was employed, SnS microspheres aggregated by nanorods were formed. Possible mechanisms for the formation of 3D SnS microstructures were proposed. Optical properties of the products were also studied.

1. Introduction

The design and synthesis of large-scale self-assembly of meso-, micro- and nanostructured building components have received considerable attention in nanoscience and nanotechnology due to their unique size, shaped-dependent properties and practical applications. A variety of complex structures, especially three-dimensional (3D) self-assembling patterns of inorganic crystals with naturally inspired morphologies such as flower-like [1,2], dendritic-like [3,4], sheaf-like [5], peanut-like (or dumbbell-like) [6–11] and olivary [12] structures have been produced. Most of the patterns were organized by nanorods or zero-dimensional nanoparticles as building units. Templates or surfactants are usually required to control oriented growth of building units. However, the introduction of the templates and surfactants increases the production cost. So the development of simple and template-free methods for creating novel microstructure patterns which may have striking properties is very important to the potential studies of physical and chemical properties of materials and is still challenge to materials scientists.

Tin monosulfide (SnS), a promising optoelectronic material with narrow band gap varying from 1.0 to 1.5 eV depending on the preparation technique and the density of states of valence band and conduction band, has received significant attention for being potential candidate in solar absorber in thin film solar cell and near infrared detector, photovoltaic materials and in holographic registrar system [13]. These applications have stimulated the search for convenient synthetic methodologies to make SnS with unique structures and well-defined optical properties. Recently, many methods were developed to fabricate SnS with various morphologies, including SnS nanorods and nanosheets [13], quantum dots [14], nanoflowers [15], dendritic-like structures [16] and thin film [17]. To our knowledge, little work has been conducted of the flowerlike SnS microstructures assembled by nanobelt-based building units.

Recently, the syntheses of semiconductor nanocrystals through a single-source precursor route have attracted much attention because of its potential advantages and possibility to tune the size and size distribution of the products by controlling the reaction conditions [18–24]. Those precursors were usually metal complexes and prepared based on the reaction of metal salt and ligands. In this work, we prepared 3D flowerlike SnS superstructures aggregated by nanoribbons, nanosheets and nanorods, and dispersed SnS lamellae by varying the ratios of $SnCl_2$ to xanthate ligand, which was previously used as raw materials to synthesize single-source precursors.

* Corresponding author. Tel.: +86 25 84315054; fax: +86 25 84315054.
E-mail addresses: qiaofenghan@yahoo.com (Q. Han), wangx@mail.njust.edu.cn (X. Wang).

0925-8388/$ – see front matter © 2010 Elsevier B.V. All rights reserved.
doi:10.1016/j.jallcom.2010.10.182

Table 1
Experimental parameters for typical samples and their morphologies.

Sample	Experimental parameters	Morphologies
1	160 °C, 24 h, $C_2H_5OCSSK/SnCl_2$ ratio is 2.4	Rose-like flowers
2	180 °C, 24 h, $C_2H_5OCSSK/SnCl_2$ ratio is 2.4	Nanobelt-based flowers
3	180 °C, 6 h, $C_2H_5OCSSK/SnCl_2$ ratio is 2.4	Nanorod-based flowers
4	180 °C, 48 h, $C_2H_5OCSSK/SnCl_2$ ratio is 2.4	Dispersed nanorods
5	180 °C, 24 h, $C_2H_5OCSSK/SnCl_2$ ratio is 2	Lamellars
6	$C_2H_5OCSSK/SnCl_2$ ratio is 2, 1 mL $C_{17}H_{33}COOK$	Nanorod-based flowers

2. Experimental

2.1. Preparation

All the reactants and solvents were of analytical grade and used without further purification. Potassium *O*-ethyldithiocarbonate (ethylxanthate, C_2H_5OCSSK) was purchased from Shanghai Chemical Co. 0.7 mmol of $SnCl_2{\cdot}2H_2O$ and 1.7 mmol of C_2H_5OCSSK were dissolved separately in 20 mL of DMF with stirring to form a homogeneous solution. Then the two solutions were mixed together in a Teflon-lined autoclave of 50 mL capacity and maintained constantly at 180 °C for 24 h. When the reactions completed, the products were filtered and washed with water and absolute alcohol for several times, and then dried under vacuum before characterization. The details about the experimental parameters for typical products and their morphologies are listed in Table 1.

2.2. Characterization

The X-ray diffraction patterns (XRD) were recorded on a Bruker D8 advanced X-ray diffractometer using Cu Kα radiation ($\lambda = 0.1542$ nm) with the range of the diffraction angle of $2\theta = 20$–80°. Transmission electron microscopy (TEM), high-resolution transmission electron microscopy (HRTEM) images were obtained on a JEM-2100 microscope (JEOL). Field emission scanning electron microscopy (FE-SEM) was taken on a LEO-1530VP scanning electron microscope equipped with a GENESIS 2000 X-ray energy spectrometer for detecting energy dispersive X-ray spectrum (EDX). The photoluminescence measurements were performed on a FL3-TCSPC fluorescence spectrophotometer using 3 nm slit width.

3. Results and discussion

Fig. 1 shows the XRD patterns of the flowerlike SnS microcrystallites assembled by nanobelts. All the reflections can be indexed to a pure orthorhombic structure of SnS (JCPDS, No: 09-0354). The strong and sharp diffraction peaks indicates that the synthesized SnS sample is well crystallized. The intensity of the peak corresponding to the (0 4 0) plane is stronger than the (1 1 1) plane, suggesting that SnS nanobelts have preferential orientation along the (0 4 0) plane [25].

Fig. 2 indicates the morphology changes of SnS particles versus reaction periods for the molar ratio of $C_2H_5OCS_2K/SnCl_2 = 2.4$ by

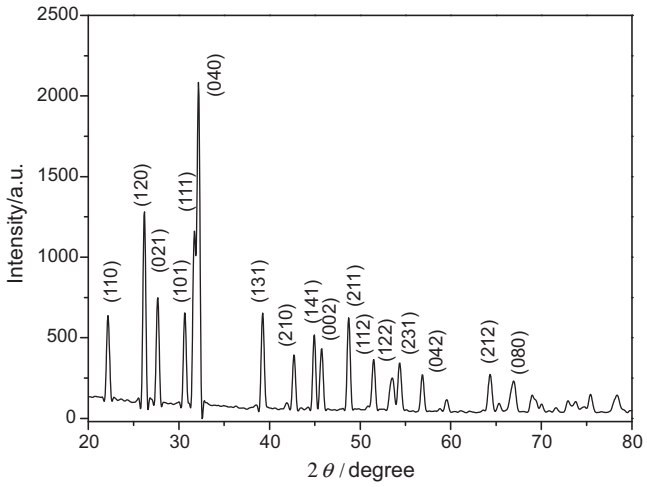

Fig. 1. XRD patterns of flowerlike SnS superstructures assembled by nanobelts.

TEM observation. At initial stage (6 h), spherical structures aggregated by irregular nanoparticles appeared. XRD results (not shown here) revealed that there was impurity $Sn(C_2H_5OCS_2)_2$ in the product. After reaction time was prolonged to 12 h, the flowerlike SnS structures consisted of nanosheets were observed (Fig. 2a). As the reaction reached 24 h, SnS beltlike structures were formed. The nanobelts grow radiately from a center toward different directions, forming flowerlike morphology, as displayed in Fig. 2b and c. The nanobelts are in a diameter of 100–200 nm and lengths up to several micrometers with sharp tips. Fig. 2d shows an HRTEM image of an individual nanobelt with atomic lattice fringes clearly visible, demonstrating that the nanobelts are highly crystallized. The regular fringes spacing of 0.28 nm is in agreement with the *d* value of (1 1 1) lattice planes of orthorhombic phase SnS. SnS beltlike structures disappeared gradually and hierarchical SnS architectures assembled by nanorods were observed when the reaction proceeded to 36 h (Fig. 2e), while dispersed nanorods are the major product for reaction duration of 48 h (Fig. 2f). Based on TEM observation at the different reaction period, we suggested a possible formation mechanism of flowerlike SnS architectures, as shown in Fig. 3. Initially, newly generated SnS nanoparticles aggregated together to form spheres driven by the minimization of the total energy of the system. With the reaction time extending, the small nanosheets would undergo relocation through dissolving and regrowing, and form larger thin sheets owing to Ostwald ripening mechanism [25]. Thin sheets rolled to form nanobelts, and finally rod-like structures. This rolling mechanism was previously reported to explain the formation of one-dimensional SnS_2 nanostructures [26].

However, if the molar ratio of potassium ethylxanthate to $SnCl_2$ was changed to 2, only distorted hexagonal SnS lamellae were produced, as shown in Fig. 4a and c. When $C_2H_5OCS_2K$ was added into $SnCl_2$ solution with the molar ratio of $C_2H_5OCS_2K/SnCl_2 = 2$, a precursor $Sn(C_2H_5OCS_2)_2$ may firstly generated and subsequently decomposed to generate SnS under solvothermal conditions. The formation of SnS nanoflakes should be a characteristic growth habit for orthorhombic SnS in solution which had been commonly reported previously [13]. If the molar ratio of $C_2H_5OCS_2K$ to $SnCl_2$ was increased to 2.4, slightly excess $C_2H_5OCS_2^-$ may act as capping reagent and coordinate to Sn^{2+} because the coordination number of Sn^{2+} is 6 [27]. This coordination interaction may control the growth rate of different crystal faces, resulting in the formation of belt-like SnS architectures. Detailed experiments of varying the molar ratios of $C_2H_5OCS_2K$ to $SnCl_2$ from 2.4 to 3 indicated that SnS superstructures composed of nanobelts formed. However, when the molar ratio of $C_2H_5OCS_2K$ to $SnCl_2$ is bigger than 3, dispersed rodlike SnS instead of SnS superstructures were obtained.

To confirm the above results that slightly excess potassium ethylxanthate could dramatically change the morphology of SnS, 1 mL of potassium oleate ($C_{17}H_{33}COOK$) was added into 40 mL DMF solution containing $Sn(C_2H_5OCS_2)_2$ (the molar ratio of $C_2H_5OCS_2K/SnCl_2 = 2$) while keeping other reaction conditions unchanged. Although oleic acid is commonly used as capping agent in shape-controlled synthesis of inorganic nanocrystals [21,28], herein, potassium oleate was used instead because of the limited solubility of oleic acid in DMF. TEM observation showed that spherical SnS architectures assembled by nanorods were generated (Fig. 4b and d). The formation of rodlike SnS architectures should be owing to the capping ligand effect of oleate. The detailed formation mechanism of hierarchical SnS architectures under the existence of a small amount coordinating reagents is not clear and the further experiment is underway.

The effect of reaction temperature on the morphology of SnS nanostructures has also been studied. When the reaction was performed at 140 °C for 24 h with the molar ratio of $C_2H_5OCS_2K/SnCl_2 = 2.4$, spherical SnS structures with rough

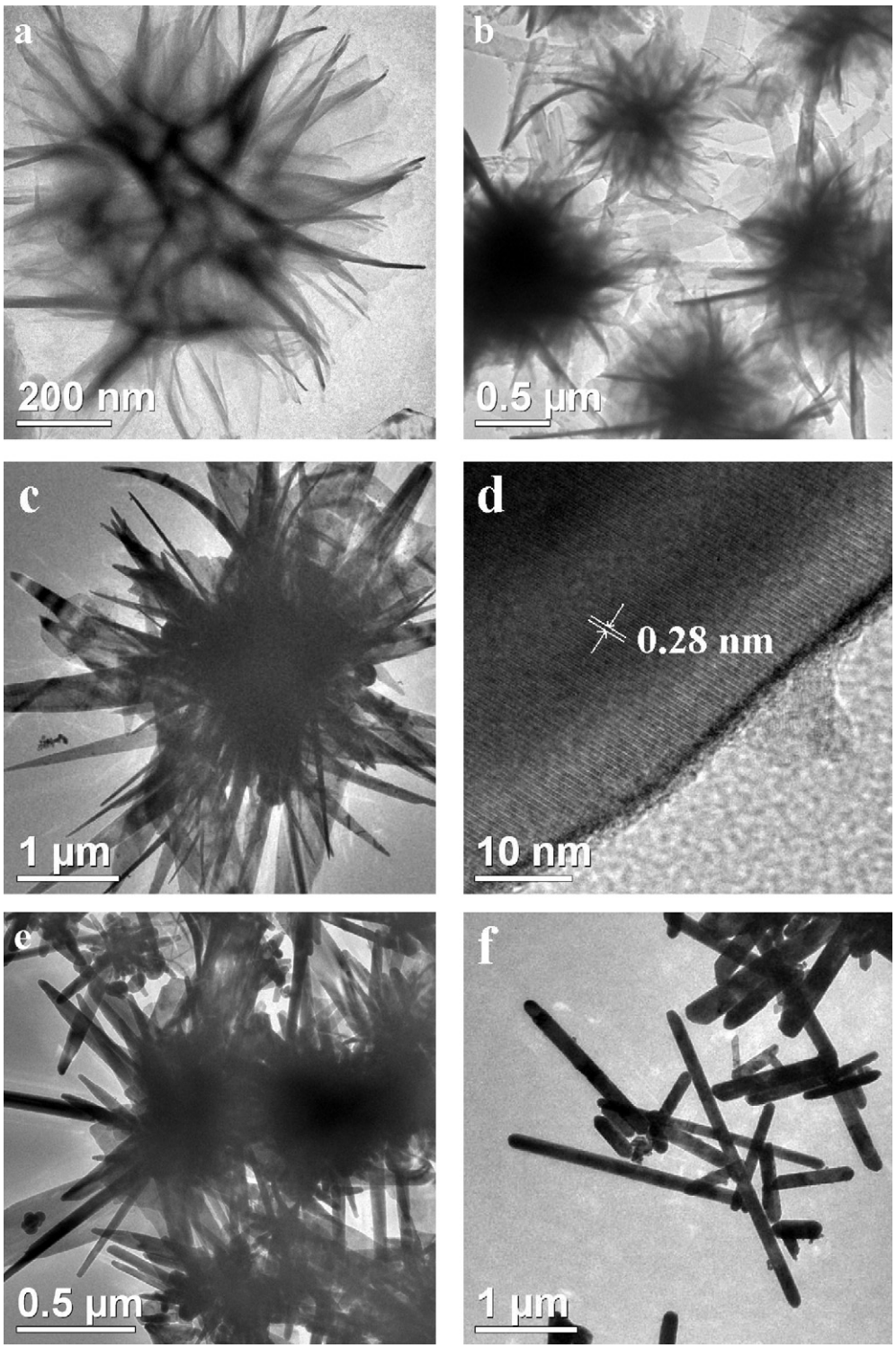

Fig. 2. TEM images of the products obtained at various reaction stages for the ratio of $C_2H_5OCS_2K/SnCl_2 = 2.4$: (a) 12 h, (b, c) 24 h, (d) HRTEM image of an individual SnS nanobelt, (e) 36 h, (f) 48 h.

surface were observed by TEM (Fig. 5a). When the reaction proceeded at 160 °C for 24 h, SnS microspheres composed of nanosheets were formed, looking like a bunched rose (Fig. 5b). The high-magnification SEM image demonstrates that hundreds of nanopetals connected with each other forming 3D hierarchical architectures, and the diameter of individual microflower is approximately 1 μm (Fig. 5c). The EDX spectrum of SnS particles demonstrates that the roselike structures are made of Sn and S with a composition close to that of the stoichiometric SnS, except for the slight excess of S (Fig. 5d). The peak assigned to platinum originates from the platinum-sputtered sample for SEM measurement and the C peak is attributed to the electric latex of the SEM sample holder.

If the concentration of $SnCl_2$ was changed from 0.7 mmol to 1.4 mmol for the molar ratio of $C_2H_5OCS_2K/SnCl_2 = 2.4$ and the reaction proceeded at 180 °C for 24 h, rod-based SnS flowers were

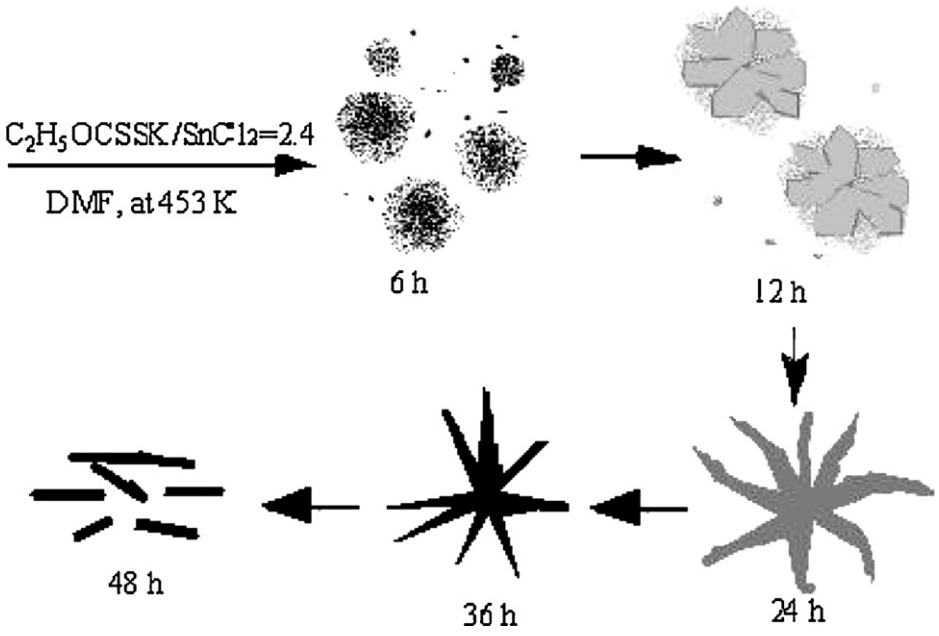

Fig. 3. A schematic illustrations for the formation of flowerlike SnS architectures composed of nanobelts.

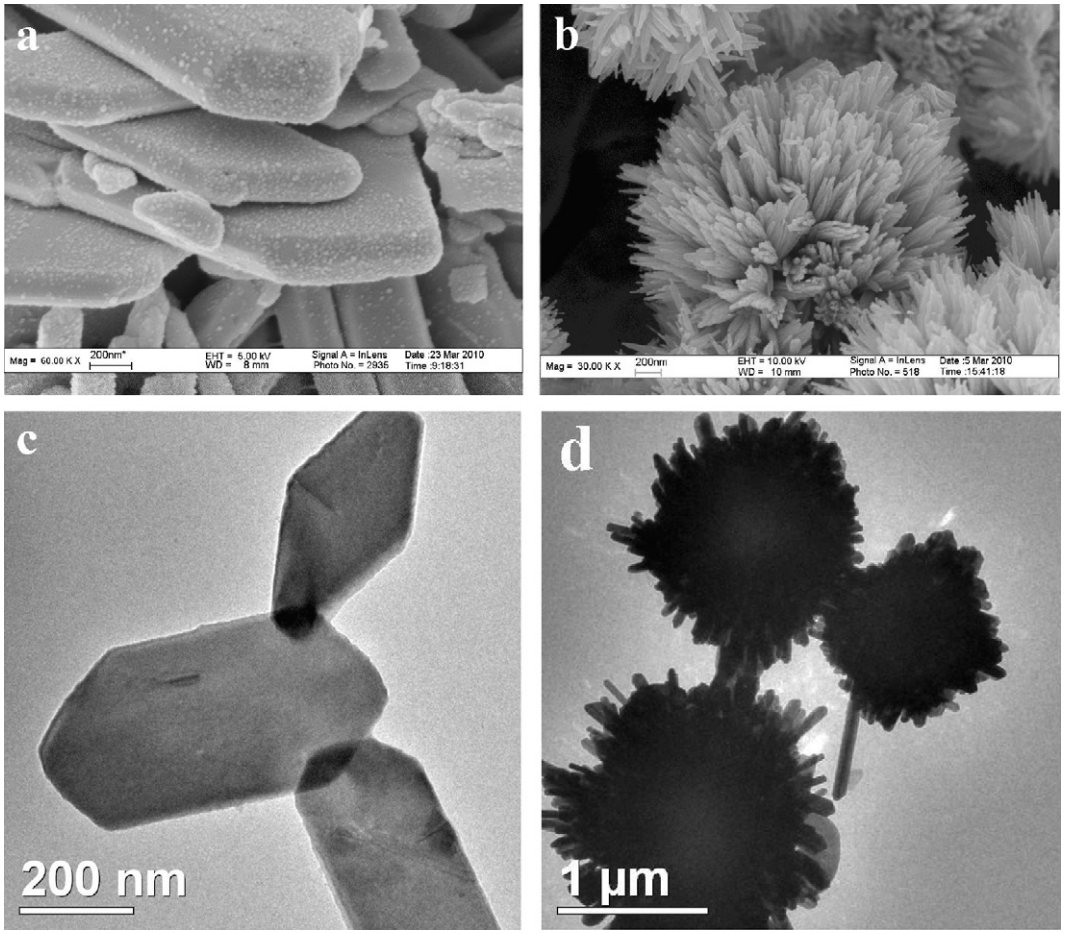

Fig. 4. SEM and TEM images of SnS obtained for the ratio of $C_2H_5OCS_2K/SnCl_2 = 2$: (a) SEM image and (c) TEM image of SnS without capping agents, (b) SEM image and (d) TEM image of SnS with 1 mL potassium oleate.

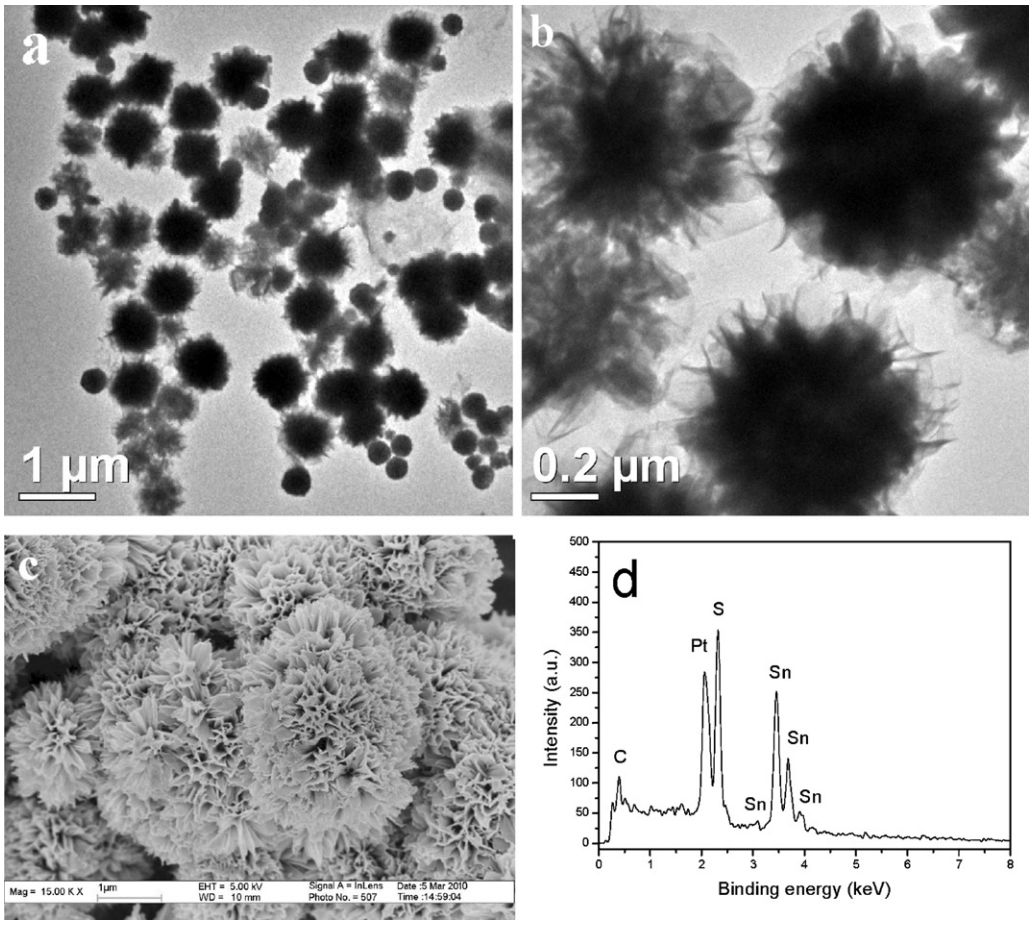

Fig. 5. TEM and SEM images of the SnS particles prepared at different temperatures: (a) TEM image of SnS prepared at 140 °C, (b) TEM image and (c) SEM image of SnS prepared at 160 °C, (d) EDX spectra of SnS prepared at 160 °C.

produced. At higher concentration, more nuclei will form at the same time and the kinetically driven growth process may be responsible for the formation of rod-based SnS structures.

The optical absorption spectra of room temperature SnS superstructures assembled by nanorods and nanobelts in ethanol are shown in Fig. 6a. The values of the optical band gap for the SnS superstructures were obtained using the equation for the near-edge absorption [29] and by the extrapolation of the liner region of the plot of $(\alpha h\nu)^2$ against photo energy $(h\nu)$ as shown in Fig. 6b. The absorption corresponds to a direct transition with a band gap of 1.3 and 1.4 eV for belt-based and rod-based SnS flowers, respectively.

Room temperature photoluminescence (PL) spectrum of the SnS hierarchical structures is shown in Fig. 7. Broad emission peak centered at about 409 nm can be observed under the excitation wavelength of 210 nm. Slight intensity difference between rod-based and belt-based SnS superstructures shows that the morphology may be responsible for PL spectra of SnS.

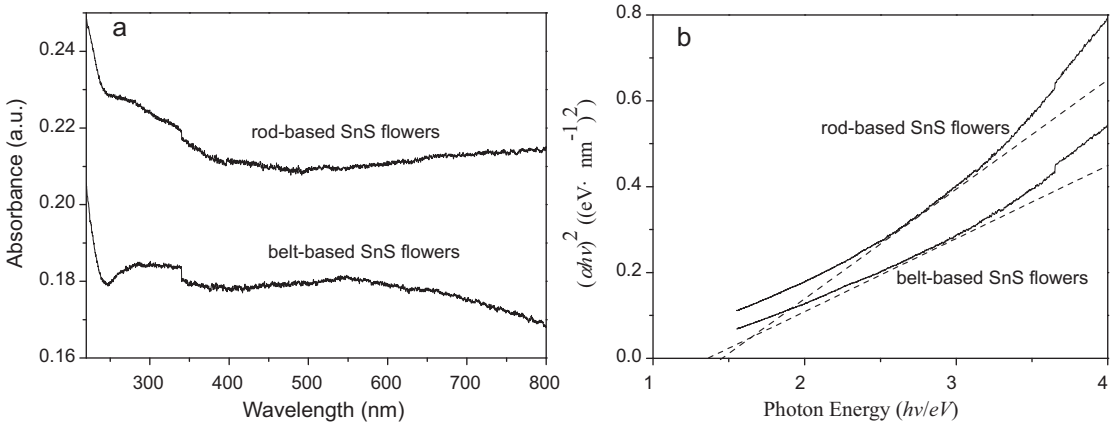

Fig. 6. (a) UV–vis absorption spectra of SnS superstructures, (b) $(\alpha h\nu)^2$ versus $h\nu$ corresponding to the direct band gap transition.

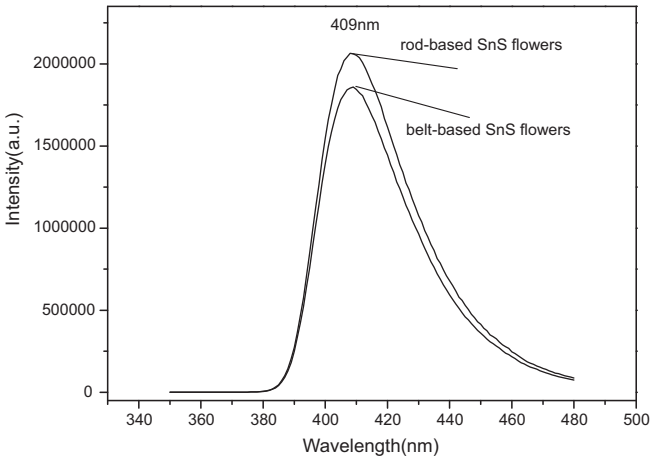

Fig. 7. Room temperature photoluminescence spectra of SnS superstructures.

4. Conclusions

In summary, hierarchical SnS architectures can be easily prepared by the addition of a small amount of capping agents such as ethyl xanthate and potassium oleate. The reaction conditions greatly influenced the morphologies of SnS nanoparticles. The absorption spectra studies show that the as-prepared SnS superstructures possess of higher band gap energy with comparison to their bulk counterparts (1.08 eV).

Acknowledgment

This work is supported by the National Natural Science Foundation of China (Grant No. 20974045) and NUST Research Funding (No. 2010GJPY042).

References

[1] B. Zhang, X. Ye, W. Hou, Y. Zhao, Y. Xie, J. Phys. Chem. B 110 (2006) 8978.
[2] J. Ota, P. Roy, S.K. Srivastava, B.B. Nayak, A.K. Saxena, Cryst. Growth Des. 8 (2008) 2019.
[3] H. Hu, Z. Liu, B. Yang, M. Mo, Q. Li, W. Yu, J. Cryst. Growth 262 (2004) 375.
[4] L. Zhou, W. Wang, H. Xu, Cryst. Growth Des. 8 (2008) 728.
[5] J. Tang, A.P. Alivisatos, Nano Lett. 6 (2006) 2701.
[6] Q.X. Wang, F. Gao, S.X. Li, W. Weng, Z.S. Hu, Chin. Chem. Lett. 19 (2008) 585.
[7] H. Cölfen, L. Qi, Chem. Eur. J. 7 (2001) 106.
[8] R. Kniep, S. Busch, Angew. Chem. Int. Ed. Engl. 35 (1996) 2623.
[9] L. Zhang, J.C. Yu, A.W. Xu, Q. Li, K.W. Kwong, S.H. Yu, J. Cryst. Growth 266 (2004) 545.
[10] M. Wang, Q.L. Huang, H.X. Zhong, X.T. Chen, Z.L. Xue, X.Z. You, Cryst. Growth Des. 7 (2007) 2106.
[11] Q. Lu, H. Zeng, Z. Wang, X. Cao, L. Zhang, Nanotechnology 17 (2006) 2098.
[12] Q. Han, J. Lu, X. Yang, L. Lu, X. Wang, Cryst. Growth Des. 8 (2008) 395.
[13] S. Biswas, S. Kar, S. Chaudhuri, Appl. Surf. Sci. 253 (2007) 9259.
[14] Y. Xu, N. Al-Salim, C.B. Bumby, R.D. Tilly, J. Am. Chem. Soc. 131 (2009) 15990.
[15] H. Zhu, D. Yang, H. Zhang, Mater. Lett. 60 (2006) 2686.
[16] H. Tang, J. Yu, X. Zhao, J. Alloys Compd. 460 (2008) 513.
[17] S. Cheng, Y. He, G. Chen, E.C. Cho, G. Conibeer, Surf. Coat. Technol. 202 (2008) 6070.
[18] O.C. Monteiro, H.I.S. Nogueira, T. Trindade, Chem. Mater. 13 (2001) 2103.
[19] W.J. Lou, M. Chen, X.B. Wang, W.M. Liu, Chem. Mater. 19 (2007) 872.
[20] Q. Han, Y. Sun, X. Wang, L. Chen, X. Yang, L. Lu, J. Alloys Compd. 481 (2009) 520.
[21] Z. Chen, Q. Tian, Y. Song, J. Yang, J. Hu, J. Alloys Compd. 506 (2010) 804.
[22] M.S. Niasari, F. Davar, A. Khansari, J. Alloys Compd. 509 (2011) 61.
[23] M.S. Niasari, A. Sobhani, F. Davar, J. Alloys Compd. 507 (2010) 77.
[24] K. Li, Q. Wang, X. Cheng, T. Lv, T. Ying, J. Alloys Compd. 504 (2010) L31.
[25] W. Ostwald, Z. Phys. Chem. 34 (1900) 495.
[26] D. Ma, H. Zhou, J. Zhang, Y. Qian, Mater. Chem. Phys. 111 (2008) 391.
[27] D.C. Menezes, G.M. de Lima, F.A. Carvalho, M.G. Coelho, A.O. Porto, R. Augesti, J.D. Ardisson, Appl. Organometal. Chem. 24 (2010) 650.
[28] C.T. Dinh, T.D. Nguyen, F. Kleitzz, T.O. Do, ACS Nano 3 (2009) 3737.
[29] D.S. Koktysh, J.R. McBride, R.D. Geil, B.W. Schmidt, B.R. Rogers, S.J. Rosenthal, Mater. Sci. Eng. B 170 (2010) 117.